

Dimensionality effect on stress in granular packings

James W. Landry,* Gary S. Grest, and Steven J. Plimpton
Sandia National Laboratories, Albuquerque, New Mexico 87185

(Dated: February 7, 2020)

The transition from two-dimensional ($2D$) to three-dimensional ($3D$) granular packings is studied using large-scale discrete element computer simulations. We focus on vertical stress profiles and examine how they change with dimensionality from $2D$ to $3D$. We compare results for packings in $2D$, quasi- $2D$ packings between flat plates, and $3D$ packings. Analysis of these packings suggests that the Janssen theory does not fully describe these packings, especially at the top of the piles, where a hydrostatic-like region of vertical stress is visible in all cases. We find that the interior of the packing is far from incipient failure, while in general, the forces at the walls are close to incipient failure.

I. INTRODUCTION

The stress within a silo packed with granular material has long been of interest in the engineering [1, 2] and physics [3] communities. As early as 1895, Janssen, in his pioneering work, constructed a model to describe the vertical stress in a silo [2]. Treating the granular pack as a continuous medium where a fraction κ of vertical stress is converted to horizontal stress, Janssen was able to derive a simple functional form for the vertical stress. One main assumption of this model is that the forces of friction between particles and walls are at the Coulomb failure criterion: $F_t = \mu_w F_n$, where F_t is the magnitude of the tangential friction force, F_n is the normal force at the wall, and μ_w is the coefficient of friction for particle-wall contacts. This assumption is also known as incipient failure. This theory qualitatively describes the crossover to a depth-independent vertical stress, although quantitative discrepancies between the Janssen theory and experiment have been observed. Numerous improvements have been added over time, but none of these have gained wide acceptance [1]. Recently, experiments have been carried out on granular packs in silos to test the suitability of Janssen's theory in ideal conditions [4, 5]. Vanel and Clément [5] constructed their initial packings by tapping a loose poured packing to increase its density. The base of the packing was then slowly moved downward to more fully mobilize the grains, and then the packing was allowed to settle. They measured the apparent mass at the bottom of the silo as a function of the filling mass of the silo. Their experiment did not follow the Janssen form, and they found the best agreement with a phenomenological theory, which contains elements of Janssen's original model. We describe this model in more detail in Sec III. Other more recent experimental studies [6, 7] have found agreement with the Janssen form. In both of these experiments, the side walls were dragged downward to fully mobilize the packing.

A variety of discrete element and continuous finite element simulation methods have been developed to describe the stresses on the walls of a silo. Most discrete element simulations thus far have been confined to two dimensional ($2D$) systems. However, there is wide disagreement between the predictive power of these models and the proper approach to take for accurate simulation [8, 9, 10, 11]. Those simulations that are carried out in three dimensions ($3D$) usually do so via finite-element methods that yield little information on the internal structure or forces in granular packs [12, 13]. The $3D$ discrete-element simulations that have been performed use periodic boundary conditions in the two directions perpendicular to gravity. Though these studies provide useful information on the internal structure of these packings [14, 15], they can give no information on vertical stresses or forces induced by the walls of the container.

Here we present large-scale discrete-element, molecular dynamics simulations of granular packings in $2D$, quasi- $2D$, and $3D$ containers (silos). Our aim is to understand the vertical stress profiles of these granular packings, particularly the crossover from two to three dimensions. Both monodisperse and polydisperse particle systems are studied. We evaluate the suitability of the Janssen theory to the observed vertical stress profiles and test the validity of its assumptions. We find that the interior of the packing is far from incipient failure, while in general, the forces at the walls are close to incipient failure. In all cases, there is a region at the top of the pile where the particle-wall forces are far from incipient failure and the Janssen form is not observed.

Section II discusses the simulation technique and the method used to generate the packings. Section III presents the vertical stress profiles. We discuss their characteristics and compare our results to the classical theory of Janssen

*Electronic address: jwlandr@sandia.gov

as well as two modified forms of the Janssen analysis. We conclude and summarize the work in Section IV.

II. SIMULATION METHOD

We present discrete-element molecular dynamics (MD) simulations in two and three dimensions of model systems of N mono- and poly-dispersed spheres of fixed density ρ . The mass of a given particle is $m_i = \frac{\rho}{6}\pi d_i^3$, where d_i is the diameter of a given particle. Particle diameters are uniformly distributed between $\bar{d} \pm \Delta$. For this study, we use $\Delta/\bar{d} = 0, 0.1, \text{ and } 0.5$. N varies from 10,000 to 50,000 particles. The system is constrained by either an open rectangular box or an open cylinder with its axis along the vertical z direction. The box has length L , width W , and height H , centered at $x = y = 0$ and bounded below with a flat base at $z = 0$. The cylinder has radius R and is centered on $x = y = 0$. It is bounded below with a flat base at $z = 0$. In some cases, a layer of randomly-arranged immobilized particles approximately $2d$ high were used to provide a rough base. We vary the length L and width W of the box and the radius R of the cylinder. This work builds on previous 3D simulations of packings in a cylinder [16].

The spheres interact only on contact through a spring-dashpot interaction in the normal and tangential directions to their lines of centers. Contacting spheres i and j positioned at \mathbf{r}_i and \mathbf{r}_j experience a relative normal compression $\delta = |\mathbf{r}_{ij} - d|$, where $\mathbf{r}_{ij} = \mathbf{r}_i - \mathbf{r}_j$, which results in a force [17]

$$\mathbf{F}_{ij} = \mathbf{F}_n + \mathbf{F}_t. \quad (1)$$

The normal and tangential contact forces are given by

$$\mathbf{F}_n = f(\delta/d)(k_n \delta \mathbf{n}_{ij} - m_{eff} \gamma_n \mathbf{v}_n) \quad (2)$$

$$\mathbf{F}_t = f(\delta/d)(-k_t \Delta \mathbf{s}_t - m_{eff} \gamma_t \mathbf{v}_t) \quad (3)$$

where $\mathbf{n}_{ij} = \mathbf{r}_{ij}/r_{ij}$, with $r_{ij} = |\mathbf{r}_{ij}|$. \mathbf{v}_n and \mathbf{v}_t are the normal and tangential components of the relative surface velocity, and $k_{n,t}$ and $\gamma_{n,t}$ are elastic and viscoelastic constants, respectively. $m_{eff} = \frac{m_i m_j}{m_i + m_j}$ for interactions between particles i and j , and $m_{eff} = m_i$ for interactions between particle i and a wall, where the mass of the wall is assumed to be infinite. $f(x) = 1$ for Hookean (linear) contacts, while for Hertzian contacts $f(x) = x^{D/2-1}$ — the two force models differing only in 3D. $\Delta \mathbf{s}_t$ is the elastic tangential displacement between spheres, obtained by integrating tangential relative velocities during elastic deformation for the lifetime of the contact. The magnitude of $\Delta \mathbf{s}_t$ is truncated as necessary to satisfy a local Coulomb yield criterion $F_t \leq \mu F_n$, where $F_t \equiv |\mathbf{F}_t|$ and $F_n \equiv |\mathbf{F}_n|$ and μ is the particle-particle friction coefficient. Frictionless spheres correspond to $\mu = 0$. Particle-wall interactions are treated identically, though the particle-wall friction coefficient μ_w is set independently. A more detailed description of the model is available elsewhere [18]. We also tested an alternate form of the F_t force due to Haff and Werner [19] that does not have history effects. This model produces a hydrostatic stress profile in all cases. Without the relative transverse displacement in the force model, $F_t = 0$ in the quasi-static limit and the walls cannot support stress.

We present all the physical quantities in our simulations in terms of \bar{d} , the average diameter; \bar{m} the mass of a particle with average diameter \bar{d} ; and g , the force of gravity. Most of these simulations were run with $k_n = 2 \times 10^5 \bar{m}g/\bar{d}$, $k_t = \frac{2}{7}k_n$, and $\gamma_n = 50\sqrt{g/\bar{d}}$. For Hookean springs we set $\gamma_t = 0$. In this case, the coefficient of restitution for $\Delta = 0$ is $\epsilon = 0.8$. For Hertzian springs, $\gamma_t = \gamma_n$. For Hertzian springs in $D = 3$, $\epsilon \rightarrow 0$ as $v \rightarrow 0$, so that it takes much longer for energy to drain out of the pack and for the kinetic energy per particle to decrease to sufficiently low levels. For this reason, it is much more computationally expensive to use Hertzian springs to form packings. The convenient time unit is $\tau = \sqrt{\bar{d}/g}$, the time it takes a particle to fall its radius from rest under gravity. For this set of parameters, the time step $\delta t = 10^{-4}\tau$. In most simulations, the particle-particle friction and particle-wall friction are the same, $\mu = \mu_w = 0.5$.

The two-dimensional (2D) simulations were performed by fixing $y = 0$ for all particles and removing any velocity or acceleration components in the y direction. Some polydispersity ($\Delta/\bar{d} > 0$) is required to prevent crystallization in 2D, so all 2D simulations were run with a polydispersity of $\Delta/\bar{d} = 0.1$.

All of our results will be given in dimensionless units based on \bar{m} , \bar{d} , and g . Physical experiments often use glass spheres of $\bar{d} = 100\mu\text{m}$ with $\rho = 2 \times 10^3 \text{kg}/\text{m}^3$. In this case, the physical elastic constant would be $k_{glass} \sim 10^{10} \bar{m}g/\bar{d}$. A spring constant this high would be prohibitively computationally expensive, because the time step must have the form $\delta t \propto k^{-\frac{1}{2}}$ for collisions to be modeled effectively. We have found that increasing k in our simulations does not appreciatively change the physical results [18].

We generate our packings by mimicking the pouring of particles at a fixed height Z into the container. For computational efficiency a group of M particles is added to the simulation on a single time step. This is done by

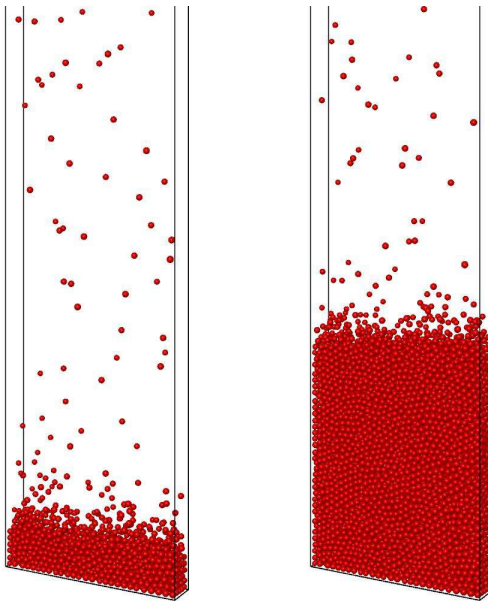


FIG. 1: Formation of a packing of $N = 10,000$ spheres in a rectangular container of length $30\bar{d}$ and width $5\bar{d}$. The black lines show the container walls. The packing is constructed by pouring from a height of $401\bar{d}$. The configurations shown represent early times and late times.

inserting the M particles at non-overlapping positions within a thin cylindrical region of radius $R - \bar{d}$ with height $Z - \bar{d} < z < Z$. The x , y , and z coordinates of the particles are chosen randomly within this insertion region. The height of insertion z determines the initial z -velocity v_z of the particle — v_z is set to the value it would have after falling from a height Z . After a time $\sqrt{2}\tau$, another group of M particles is inserted. This methodology generates a steady stream of particles, as if they were poured continuously from a hopper (see Figure 1). The rate of pouring is controlled by setting M to correspond to a desired volume fraction of particles within the insertion region. For example, for an initial volume fraction of $\phi_i = 0.13$ in a cylinder of $R = 10\bar{d}$, the pouring rate is ≈ 45 particles/ τ . This method is similar to the homogeneous “raining” methods used in experiments [20].

The simulations were run until the kinetic energy per particle was less than $10^{-8}\bar{m}g\bar{d}$. The resultant packing is considered quiescent and used for further analysis [15]. In 3D, Hertzian packings have difficulty reaching this criteria due to long-lived pressure waves that traverse the entire pile. In these packings, the kinetic energy per particle tends to stabilize at approximately $10^{-3}\bar{m}g\bar{d}$ for very long times. By adding a viscous damping term proportional to v after the pack has stabilized at $10^{-3}\bar{m}g\bar{d}$, we were able to reduce the kinetic energy per particle of these systems to less than $10^{-8}\bar{m}g\bar{d}$. A comparison of the stress profiles before and after the application of this viscous damping term showed no change. Although a change of kinetic energy of this order has a small effect on the coordination number of the packing, it does not have any effect on the vertical stress. All vertical stress profiles for Hertzian packings presented in the following sections were generated with this technique.

These simulations were performed on a parallel cluster computer built with DEC Alpha processors and Myrinet interconnects using a parallel simulation code optimized for short-range interactions [18, 21]. A typical simulation to pour 50,000 particles into a 3D cylindrical silo requires 5×10^6 time steps, which requires roughly 40 CPU hours on each of 50 processors.

We show in Figure 1 how a typical packing is created. The figure shows three snapshots in time as particles are poured into a quasi-2D system of length $30\bar{d}$ and width $5\bar{d}$.

III. STRESSES

Of particular interest in the construction of silos is the distribution of stresses [1]. In a liquid, hydrostatic pressure increases with depth. Granular materials support shear, so the side walls of a container can support some of this shear, provided $\mu_w > 0$. The problem of the resultant vertical stress in a silo after filling has a long history, beginning with Janssen in 1895. Janssen’s analysis[2, 22] is still in use today, although it rests on a series of assumptions which have not been fully tested.

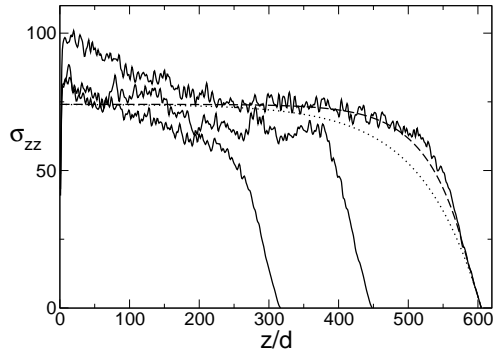


FIG. 2: Vertical stress σ_{zz} for $2D$ packings. The packings in order of decreasing depth are (a) $N \approx 20000$, length $L = 30\bar{d}$, (b) $N \approx 10000$, $L = 20\bar{d}$, and (c) $N \approx 10000$, $L = 30\bar{d}$. The particles are polydisperse with $\Delta = 0.1\bar{d}$. The two fits to (a) are a fit to Janssen (Eqn. 4) (dotted line) and a fit to Vanel-Clément (Eqn. 5) (dashed line).

For a container with static wall friction μ_w and granular pack of total height z_0 , the Janssen analysis predicts the vertical stress $\sigma_{zz}(z)$ at a height z is

$$\sigma_{zz}(z) = \rho g l \left[1 - \exp\left(-\frac{z_0 - z}{l}\right) \right] \quad (4)$$

where ρ is the volumetric density, l is the decay length, and z_0 is the top of the packing. The decay length l is determined by the geometry. For a $2D$ container of length L , $l_{2D} = \frac{L}{2\kappa\mu_w}$. For a quasi- $2D$ container of length L and width W , $l_{quasi-2D} = \frac{LW}{2L+2W} \frac{1}{\kappa\mu_w}$. For a $3D$ cylindrical container of radius R , $l_{3D} = \frac{R}{2\kappa\mu_w}$ [23].

Another two-parameter fit was proposed by Vanel and Clément [4] to reconcile their experimental findings on weakly shaken packings with Janssen theory. The fit assumes a region of perfect hydrostaticity, followed by a region that conforms to the Janssen theory.

$$\begin{aligned} z_0 - z < a & : \sigma_{zz}(z) = \rho g(z_0 - z) \\ z_0 - z > a & : \sigma_{zz}(z) = \rho g \left(a + l \left[1 - \exp\left(-\frac{z_0 - z - a}{l}\right) \right] \right) \end{aligned} \quad (5)$$

The two parameters are a , the height of the crossover, and l the decay length, with the same values for different geometries as in the Janssen theory.

We first present vertical stresses for the two-dimensional ($2D$) case. These are shown in Figure 2. Unlike previous studies [10], these piles are extremely deep so that the height-independent region can be easily observed. The Janssen theory does not describe the $2D$ stress profiles well. There is a clear linear hydrostatic-like region at the top of the packing that the Janssen theory does not account for. The Vanel-Clément form is a much closer fit to the data. In Figure 2, the deepest pile of length $30\bar{d}$ is fit to both forms. The Janssen form predicts $l/\bar{d} = 84.6$ and thus $\kappa = 0.354$, while the Vanel-Clement form yields $a = 35$ and $l/\bar{d} = 49.6$ and thus $\kappa = 0.605$. As we will see below, there are a number of differences between $2D$ and $3D$ packings. One difference is the height of the non-saturated region, which is on the order of $5 - 7L$ in $2D$ and $6R$ in $3D$. There is about a factor of 2 difference between the diameter or width of the container in $2D$ compared to $3D$. In addition, the saturated pressure is also much larger in $2D$ than the $3D$ case. Both of these effects seem to arise from the necessity of all the force being carried by the side walls. A similar effect is seen at the bottom of the packing, where the slight increase in the pressure at the bottom of the pile is over a much larger region than in the $3D$ case as shown below. This increase occurs because geometrically the walls can not support forces from particles below this height.

To study the crossover from $2D$ to $3D$, we studied a series of packings in rectangular containers with increasing width, ranging from $W = 1.2\bar{d}$ to $5\bar{d}$. We show in Figure 3 the vertical stress profiles for these quasi- $2D$ packings. The stress profiles show the same hydrostatic region followed by saturation as the $2D$ profiles, though the hydrostatic region at the top of the pile is much smaller in the quasi- $2D$ case. In addition, the saturation stress value does not increase monotonically with width. The saturation stress decreases as one goes from a width of $1.2\bar{d}$ to $1.4\bar{d}$, but increases again as one reaches $2\bar{d}$. A width of $2\bar{d}$ seems to represent a transition to a more $3D$ -like behavior, and the saturation stress does not change appreciably for larger widths. This suggests that L is the dominant length scale for

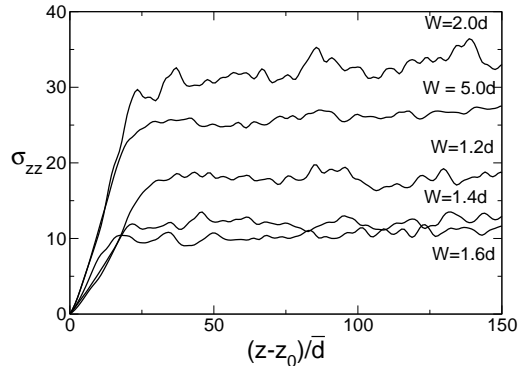


FIG. 3: Vertical stress for quasi-2D packings with increasing widths, shown as $(z - z_0)/\bar{d}$, where z_0 is the top of the pile. Six separate packings are shown, with the width W increasing from $1.2\bar{d}$ to $5.0\bar{d}$. The pressure-independent height does not increase monotonically with W , and it saturates at $W = 2.0\bar{d}$. Results for Hookean springs and polydispersity $\Delta = 0.1\bar{d}$.

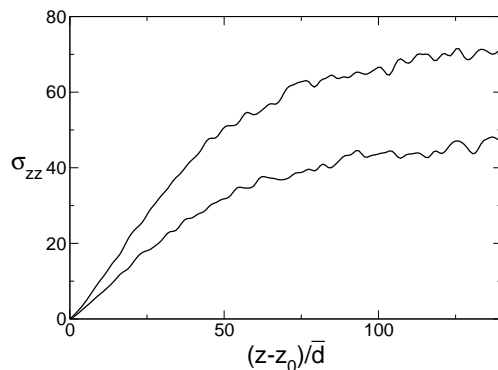


FIG. 4: Vertical stress for quasi-2D packings of length $30\bar{d}$ and width $1.6\bar{d}$ (lower curve) and width $2\bar{d}$ (upper curve). The long walls of length $L = 30\bar{d}$ have $\mu_w = 0$, while the short walls have $\mu_w = 0.5$. The stress profiles are very close to those of the 2D simulations.

widths greater than $2\bar{d}$, while for smaller widths, the width W is the dominant length scale for determination of the vertical stress.

We also investigated quasi-2D packings with no friction on the long walls $\mu_w = 0$, while the short side walls have $\mu_w = 0.5$. This system was modeled to understand how the long side walls affect the geometry. This system, as shown in Figure 4, produces stress profiles very different from the quasi-2D case with friction on all walls. Two widths were used and both show much larger final stress values and much larger hydrostatic regions. This suggests that both sets of walls are important for determining the stress profiles for a wide range of widths. The stress profiles seen in this case resemble much more the 2D stress profiles presented in Fig 2. These results demonstrate that experiments in thin plates meant to approximate 2D systems are more representative of 3D systems than that of pure 2D systems.

We show in Figure 5 vertical stress profiles for 3D systems in cylindrical packings. Changing the force model from a Hookean to a Hertzian interaction has a very small effect on the final packing. Changing from a monodisperse to a very highly polydisperse system ($\Delta/\bar{d} = 0.5$) also does not change the overall stress profile, although it does increase the height of the packing. This suggests that although polydispersity is required in 2D systems to avoid crystallization, it has little effect on the stress profile. It is thus reasonable to compare monodisperse 3D packings to polydisperse 2D systems.

In this case we see that the important transition is from the 2D system to the quasi-2D system. In most respects the quasi-2D system is much closer to the 3D system than the pure 2D system. The size of the hydrostatic region changes most markedly from the pure 2D system to the quasi-2D system. The stress values in the depth of the pile are much larger for the 2D case than the quasi-2D case and are comparable to the 3D case.

We can also test directly the Janssen assumptions of incipient failure in our simulations, i.e. whether the tangential

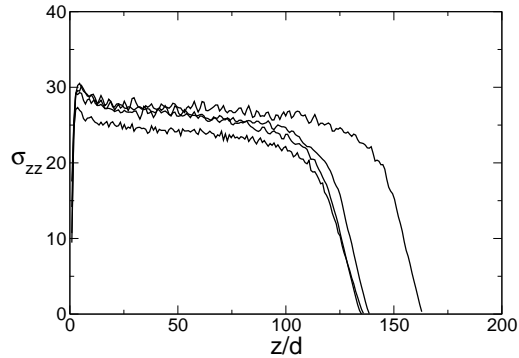


FIG. 5: Vertical stress σ_{zz} for 3D cylindrical packings with radius $10\bar{d}$ and $N = 50,000$. The four different packings are (a) a monodisperse ($\Delta = 0$) packing with Hookean contacts, (b) a monodisperse packing with Hertzian contacts, (c) a polydisperse ($\Delta/\bar{d} = 0.1$) packing with Hertzian contacts, and (d) a polydisperse ($\Delta/\bar{d} = 0.5$) packing with Hertzian contacts. The packings in order of ascending height are c, a, b, d. Results for $\mu = \mu_w = 0.5$. Results for case a are averaged over 4 runs while the other three cases are for one run each.

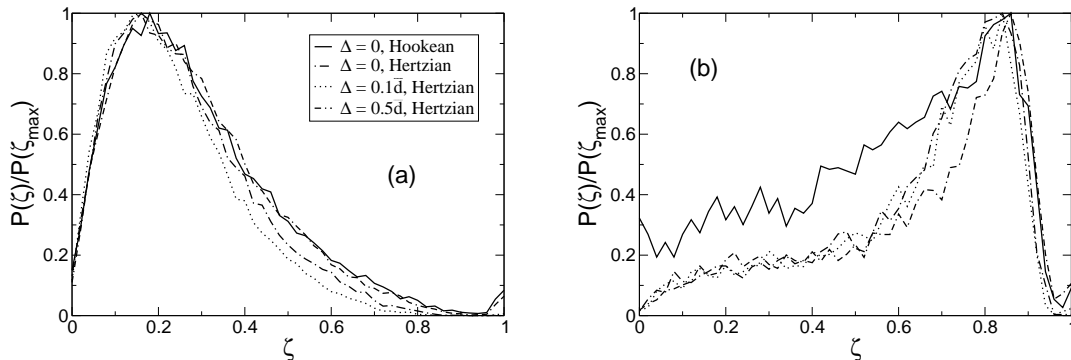


FIG. 6: Probability distributions $P(\zeta)$ in the height-independent pressure region in the bulk of the packing (a) and at the side walls (b), each normalized by its maximum value $P(\zeta_{\max})$. $\zeta = F_t/\mu F_n$ in (a) and $\zeta = F_t/\mu_w F_n$ in (b). The legend applies to both figures. Forces in the bulk are far from the Coulomb failure criterion, while those at the walls are very close to it.

forces at the wall are actually at the Coulomb yield criterion $F_t = \mu_w F_n$. We define $\zeta = F_t/\mu F_n$ in the bulk of the packing and $\zeta = F_t/\mu_w F_n$ for forces at the wall. If a specific force is at the Coulomb failure criterion, $\zeta = 1$. We analyzed the 3D systems shown in Figure 5. By examining the distribution of forces in the interior of our packings, we find that no particle-particle contacts are at the Coulomb criterion irrespective of method or level of polydispersity, as shown in Figure 6a. We find similar results in the interior of 2D packings. However the particle-wall forces in the height-independent stress region are much closer to the Coulomb criterion. In the four systems examined, the bulk of the particle-wall tangent forces are close to incipient failure, in contrast to the particle-particle tangent forces in the bulk, as seen in Figure 6b. The amount of polydispersity and the contact force model have essentially no effect on how close the system is to incipient failure. We have also investigated the role of $\mu_w > \mu$ in Ref. [16]. In this case, the particle-wall forces are always less than the Coulomb criterion, as the walls do not support larger tangential forces than those supported in the bulk.

As discussed above, all of our packings exhibit a linear region in the stress profile at the top of the packing. We can also examine the Janssen assumption in this linear region. In contrast to the situation in the height-independent stress region of the packing, near the top of the pile the forces at the wall are far from the Coulomb criterion, as shown in Figure 7. This explains why the Janssen form is not obeyed in this region: the walls in this region do not support stress and thus the stress profile is hydrostatic.

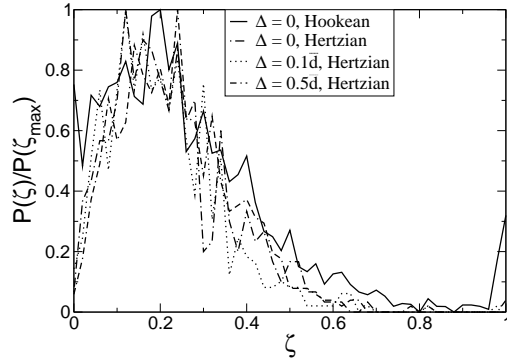


FIG. 7: Probability distributions $P(\zeta)$ at the side wall in the linear hydrostatic region at the top of the packing with $\mu = \mu_w = 0.5$, each normalized by its maximum value $P(\zeta_{\max})$. $\zeta = F_t/\mu_w F_n$. In contrast to the behavior in the height-independent pressure region, the forces at the walls are far from the Coulomb failure criterion in all cases.

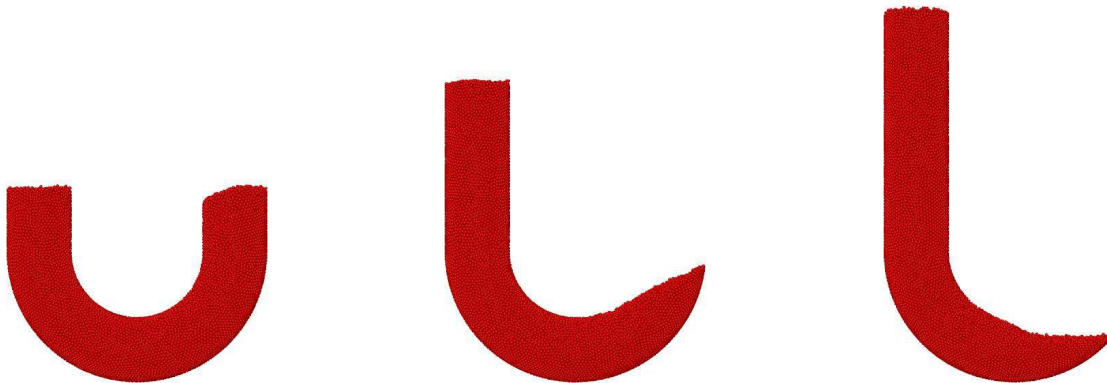


FIG. 8: Packings of $N = 10000$ particles in U-Tubes with different μ_w . Particles were poured into the left-hand side and allowed to settle into packings. a) has walls with $\mu_w = 0.0$, so there is no stress carried by the walls. b) has walls with $\mu_w = 0.1$, so the walls support slight stresses and there is a height difference between the left and right tubes. c) has walls with $\mu_w = 0.5$, and there is a great difference between the left and right tubes.

IV. CONCLUSIONS

We examined the differences between vertical stress in granular packings in $2D$, quasi- $2D$, and $3D$. We focused on the vertical stress of these packings and observed that $2D$ packings support much less vertical stress than $3D$ packings. In contrast, quasi- $2D$ packings (those packings between thin walls) rapidly converge to the behavior of $3D$ packings as the wall thickness is increased, though their progression is not monotonic. We also show that polydispersity and different force models do not have a large effect on the vertical stress in $3D$ packings. In all cases, we show that the Janssen assumption of incipient failure is not justified everywhere in the packing.

Finally, we also wish to stress the strong effect of friction on the capacity of a silo to support stress. We show in Figure 8 a demonstration of the strong effect of varying the wall friction μ_w . The geometry is that of a three-dimensional U-tube, with both ends open. Particles are poured into one end and the resultant packing is allowed to settle. In the case where $\mu_w = 0$, no stress can be supported by the side walls, and the granular packing is liquid-like: the particle height is the same in both sides of the U-tube. For $\mu_w = 0.1$, the right side is considerably lower than the left, though some particles are higher than the bend in the tube. The walls support some of the stress, but the pressure is strong enough to force some particles up the right-hand tube. For $\mu_w = \mu = 0.5$, there are almost no particles on the right side of the U-tube, and all the weight on the left side is supported by the walls of the tube.

We acknowledge discussions with L. Silbert and Jin Ooi, and thank L. Silbert for his critical reading of the manuscript. This work was supported by the Division of Materials Science and Engineering, Basic Energy Sciences, Office of Science, U.S. Department of Energy. This collaboration was performed under the auspices of the DOE Center of Excellence for the Synthesis and Processing of Advanced Materials. Sandia is a multiprogram laboratory operated by Sandia Corporation, a Lockheed Martin Company, for the United States Department of Energy under Contract DE-AC04-94AL85000.

-
- [1] R. M. Nedderman, *Statics and Kinematics of Granular Materials* (Cambridge University Press, 1992).
 - [2] H. A. Janssen, *Z. Ver. Dt. Ing* **39**, 1045 (1895).
 - [3] H. M. Jaeger, S. R. Nagel, and R. P. Behringer, *Rev. Mod. Phys.* **68**, 1259 (1996).
 - [4] L. Vanel and E. Clément, *Eur. Phys. B* **11**, 525 (1999).
 - [5] L. Vanel, P. Claudin, J.-P. Bouchaud, M. Cates, E. Clément, and J. P. Wittmer, *Phys. Rev. Lett.* **60**, 1439 (2000).
 - [6] Y. Bertho, F. Giorgiutti-Dauphiné, and J.-P. Hulin (2002), cond-mat/0211510.
 - [7] G. Ovarlez, C. Fond, and E. Clément (2002), cond-mat/0212228.
 - [8] S. Masson and J. Martinez, *Powder Tech.* **109**, 164 (2000).
 - [9] J. M. F. G. Holst, J. Y. Ooi, J. M. Rotter, and G. H. Rong, *J. Eng. Mech.* **125**, 94 (1999).
 - [10] J. M. F. G. Holst, J. Y. Ooi, J. M. Rotter, and G. H. Rong, *J. Eng. Mech.* **125**, 104 (1999).
 - [11] A. M. Sanad, J. Y. Ooi, J. M. F. G. Holst, and J. M. Rotter, *J. Eng. Mech.* **127**, 1033 (2001).
 - [12] J. F. Chen, S. K. Yu, J. Y. Ooi, and J. M. Rotter, *J. Eng. Mech.* **127**, 1058 (2001).
 - [13] D. Guines, E. Ragneau, and B. Kerour, *J. Eng. Mech.* **127**, 1051 (2001).
 - [14] H. A. Makse, D. L. Johnson, and L. M. Schwartz, *Phys. Rev. Lett.* **84**, 4160 (2000).
 - [15] L. E. Silbert, D. Ertas, G. S. Grest, T. C. Halsey, and D. Levine, *Phys. Rev. E* **65**, 031304 (2002).
 - [16] J. W. Landry, G. S. Grest, L. E. Silbert, and S. J. Plimpton (2002), cond-mat/0211218.
 - [17] P. A. Cundall and O. D. L. Strack, *Geotechnique* **29**, 47 (1979).
 - [18] L. E. Silbert, D. Ertas, G. S. Grest, T. C. Halsey, D. Levine, and S. J. Plimpton, *Phys. Rev. E* **64**, 051302 (2001).
 - [19] P. K. Haff and B. T. Werner, *Powder Technology* **48**, 239 (1986).
 - [20] L. Vanel, D. Howell, D. Clark, R. P. Behringer, and E. Clément, *Phys. Rev. E* **60**, R5040 (1999).
 - [21] S. J. Plimpton, *J. Comp. Phys.* **117**, 1 (1995).
 - [22] L. Rayleigh, *Phil. Mag. Ser. 6* **11**, 129 (1906).
 - [23] J. Duran, *Sands, Powders, and Grains: An Introduction to the Physics of Granular Materials* (Springer-Verlag, 2000).